Electronic Supplementary Information (ESI)

Highly Selective Recognition of Al^{3+} and I^- ions using a Bi-functional Fluorescent Probe

Zhao Li,‡[a] Jiang-Lin Zhao,‡[b] Yu-Tian Wu,[a] Lan Mu,[a] Xi Zeng,*[a] Zongwen Jin,*[b] Gang Wei,*[c] Ning Xie[e] and Carl Redshaw[d]

[a] *Key Laboratory of Macrocyclic and Supramolecular Chemistry of Guizhou Province, Guizhou University, Guiyang 550025, P.R. China*

[b] *Shenzhen Institutes of Advanced Technology, Chinese Academy of Sciences, 1068 Xueyuan Avenue, Shenzhen 518055, China.*

[c] *CSIRO Manufacturing, PO Box 218, NSW 2070, Australia*

[d] *Department of Chemistry, School of Mathematics & Physical Sciences, University of Hull, Hull HU6 7RX, U.K.*

[e] *College of Life Science, Shenzhen Key Laboratory of Microbial Genetic Engineering, Shenzhen University, Shenzhen 518060, China*

‡ *Zhao Li and Jiang-Lin Zhao contributed equally to this work.*

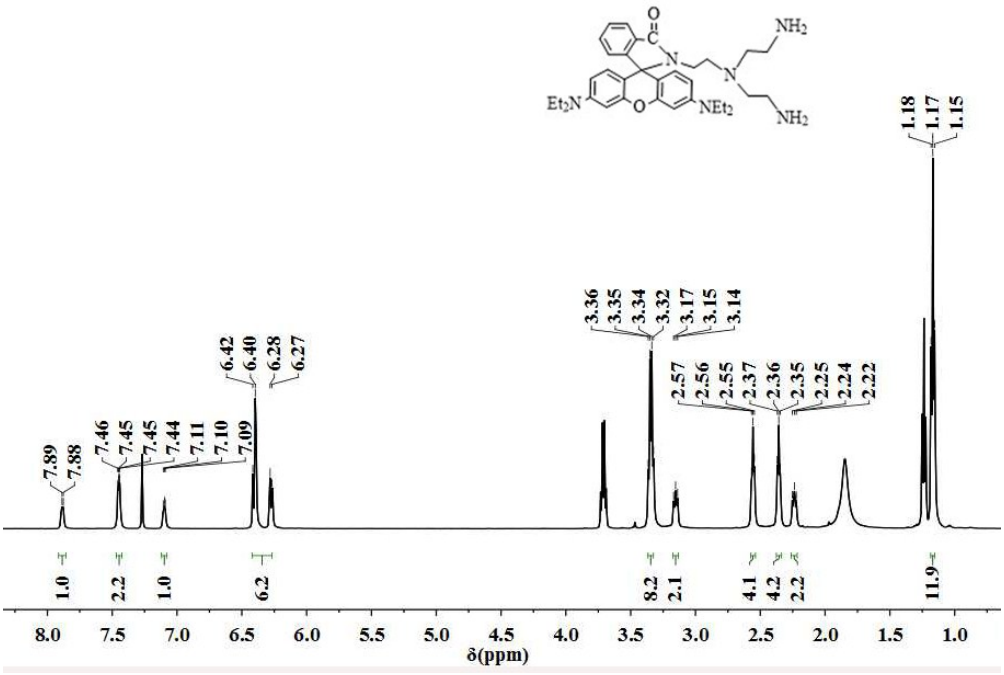

Figure S1. ^{1}H NMR spectrum of intermediate **1** (500 MHz, $CDCl_3$, 293 K).

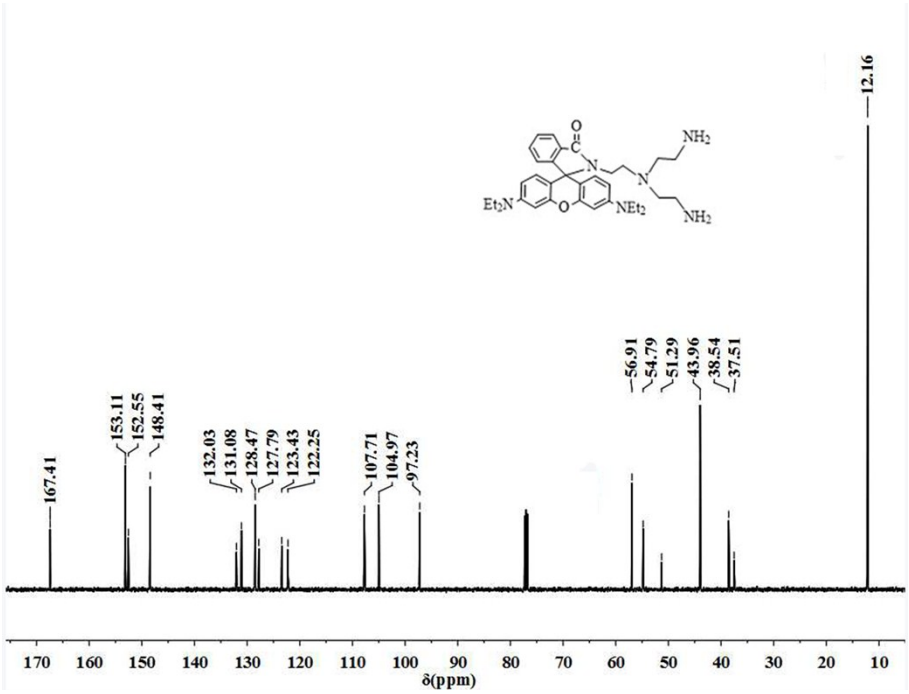

Figure S2. ^{13}C NMR spectrum of intermediate **1** (125 MHz, $CDCl_3$, 293 K).

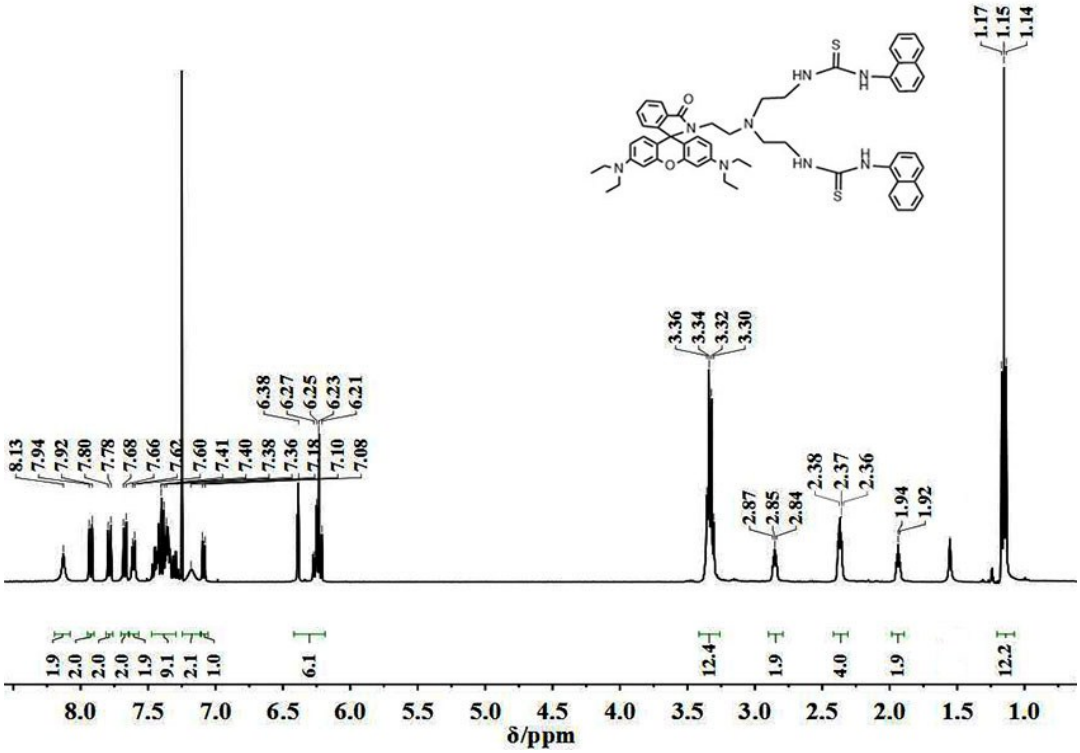

Figure S3. ^{1}H NMR spectrum of probe **L1** (500 MHz, $CDCl_3$, 293 K).

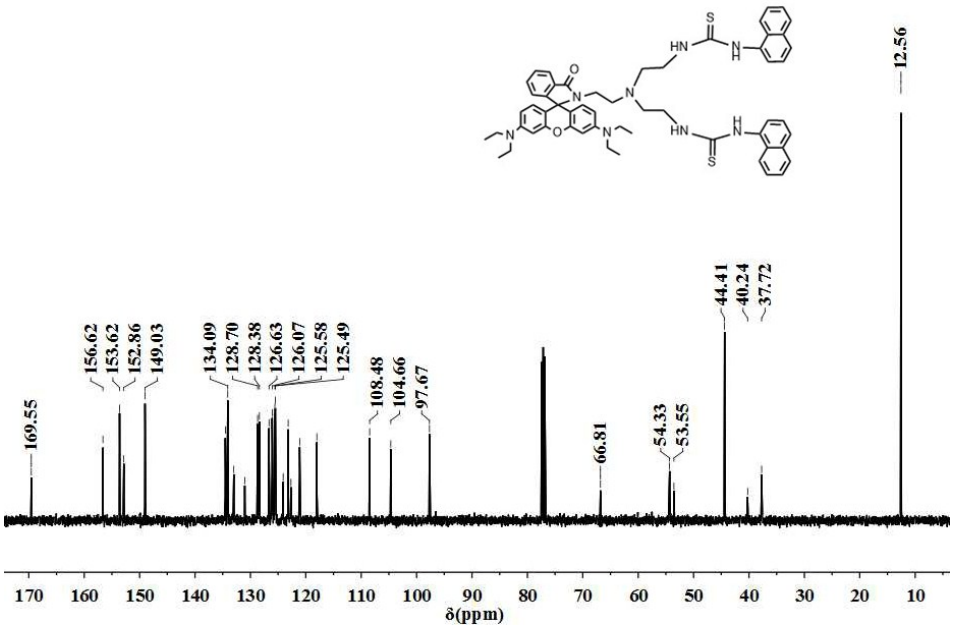

Figure S4. ^{13}C NMR spectrum of probe **L1** (125 MHz, $CDCl_3$, 293 K).

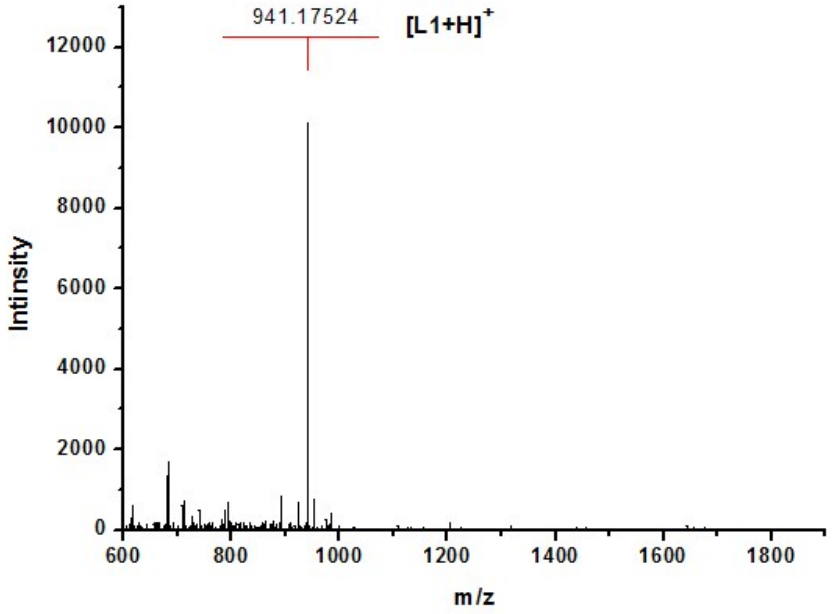

Figure S5. MALDI-TOF-MS spectrum of probe **L1**.

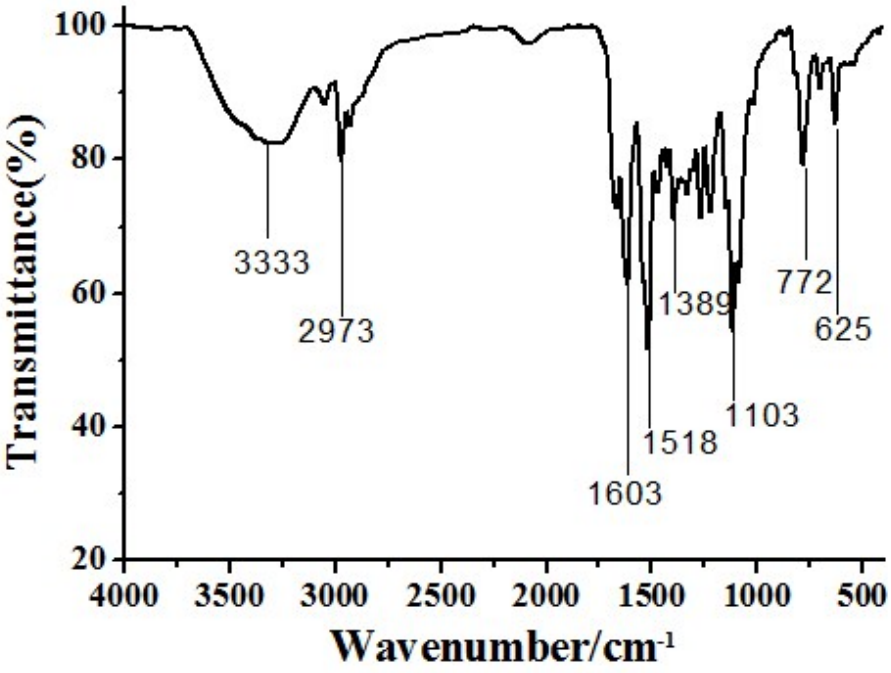

Figure S6. FT-IR spectrum of probe **L1**.

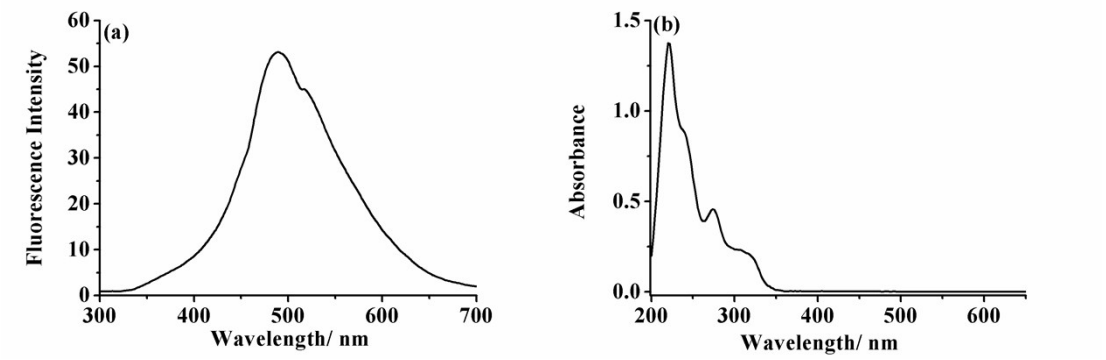

Figure S7. (a) Fluorescence spectra of probe **L1**; (b) Absorption spectra of probe **L1** (10 μM, H_2O/CH_3CN, 2/98, v/v, pH 7).

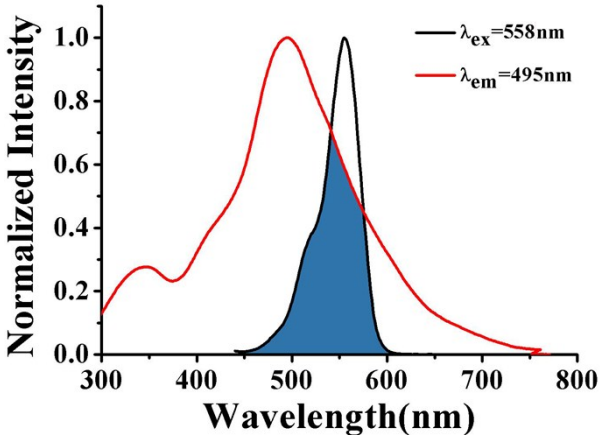

Figure S8. Spectral overlap between the energy donor naphthaline emission (black) and acceptor rhodamine absorption (red).

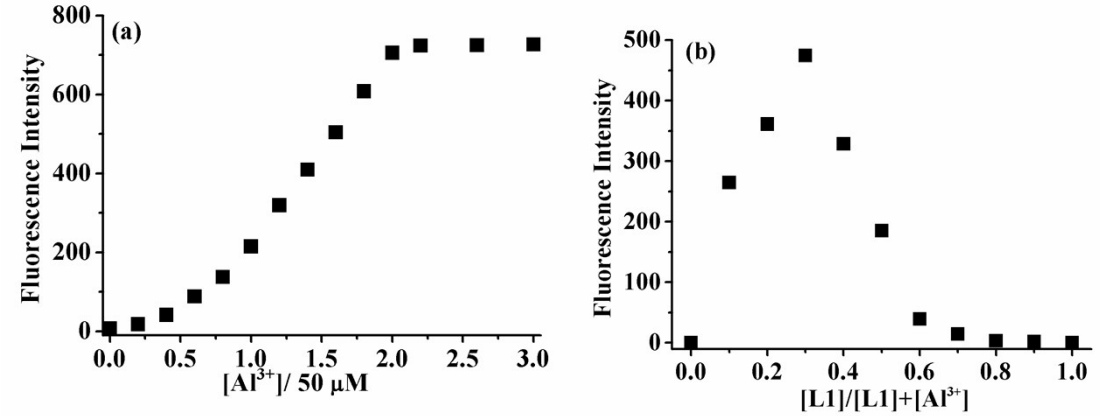

Figure S9. The plot of fluorescence intensity of probe **L1** as a function of Al^{3+} concentration (a) and the Job's plot data (b).

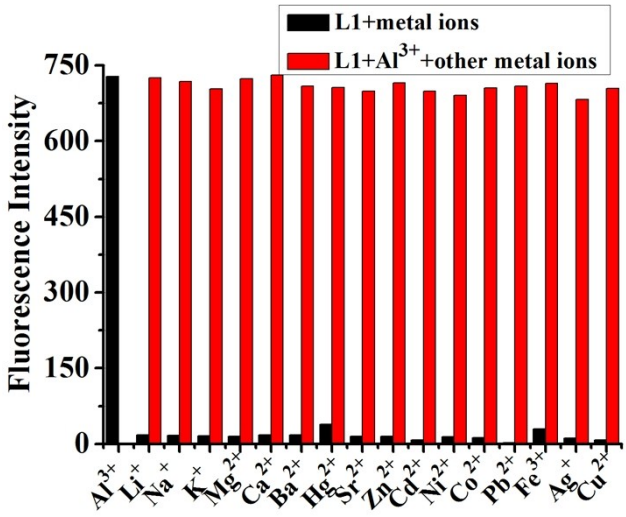

Figure S10. Fluorescence response of probe **L1** (10 μM, H_2O/CH_3CN, 2/98, v/v, pH 7). Black bars: emission intensity of probe **L1** at 585 nm with the addition of the respective metal ions (20 equiv.). Red bars: emission intensity of **L1**·$2Al^{3+}$ complex at 585 nm with the addition of the respective competing ions (20 equiv.). Metal ions including Al^{3+}, Li^{+}, Na^{+}, K^{+}, Mg^{2+}, Ca^{2+}, Ba^{2+}, Sr^{2+}, Hg^{2+}, Pb^{2+}, Cd^{2+}, Zn^{2+}, Co^{2+}, Ni^{2+}, Cu^{2+}, Ag^{+} and Fe^{3+}, λ_{ex} = 240 nm.

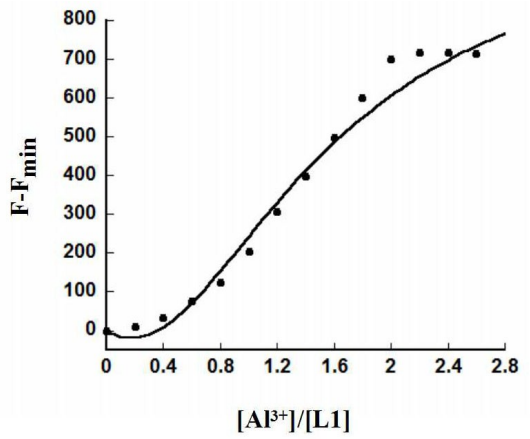

Figure S11. Non-linear plot of probe **L1** (50 μM) assuming a 1:2 stoichiometry for association between probe **L1** and Al^{3+} in CH_3CN/H_2O (v/v, 98/2, pH 7) solution by fluorescence spectroscopy; $\lambda_{ex}/\lambda_{em}$ = 240 nm/585 nm.[1]

The fluorescence spectrum association constants of Al^{3+} were calculated by nonlinear fitting using the following formula [Eq. (1)]:

$$\Delta F_{Al} = \frac{\kappa_{\Delta HG}[H_0] + \kappa_{\Delta HG\,2}[H_0]K_1K_2[G]^2}{1 + K_1[G] + K_1K_2[G]^2} \quad (1)$$

where ΔF_{Al} is the change in the fluorescence intensity of the **L1** upon gradual addition

of the Al^{3+}, $\kappa_{\Delta HG}$ refers to the different proportionality constant of the complex HG and the free host, and $\kappa_{\Delta HG_2}$ refers to the different proportionality constant of the complex HG_2 and the free host. The total concentrations of host and guest are denoted by [H] and [G], respectively.

Equation(1) is noting also the relevant mass balance eqn (2), molar concentration of the 1 : 1 complex are denoted by [HG], [HG2] refers to 1 : 2 complex[1].

$$[H0] = [H] + [HG] + [HG2] \quad (2)$$

$R = 0.9898$, $K_1 = 777.45 (\pm 0.391)\ M^{-1}$, $K_2 = 3.099 \times 10^5 (\pm 0.391)\ M^{-2}$.

Reference:
[1] P. Thordarson, *Chem. Soc. Rev.*, 2011, **40**, 1305-1323.

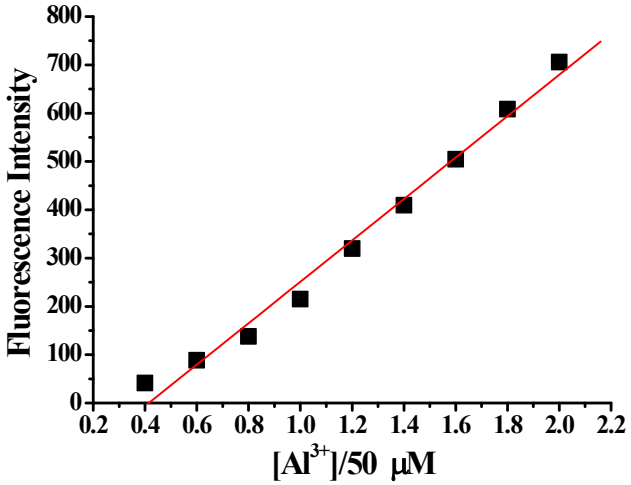

Figure S12. Fluorescence intensity calibration curve of probe **L1** (50 μM) as a function of Al^{3+} concentration in CH_3CN/H_2O (v/v, 98/2, pH 7) solution; $\lambda_{ex}/\lambda_{em}$ = 240 nm/585 nm. Y = 428.8 X - 177.8, R = 0.9935, LOD = 0.062 μM.

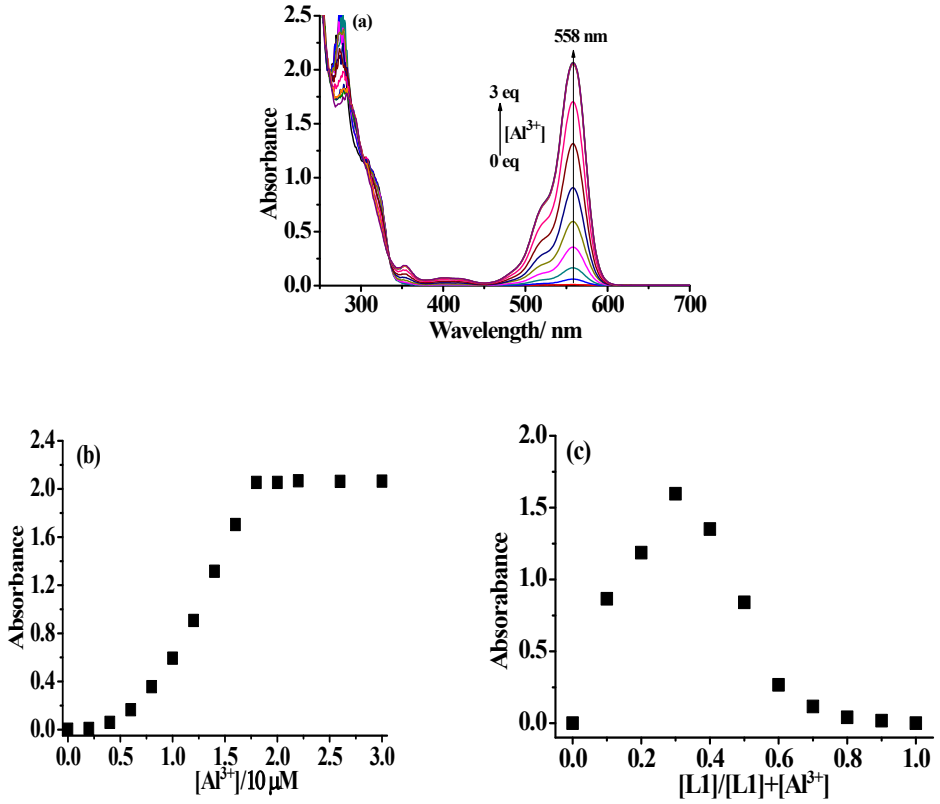

Figure S13. (a)Absorption spectral changes of probe **L1** (pH 7, 50 μM, H_2O/CH_3CN, 2/98, v/v) solution upon addition of Al^{3+} (0 ~ 30 μM); (b) the plot of absorbance at 558nm of probe **L1** as a function of Al^{3+} concentration and (c) the Job's plot data.

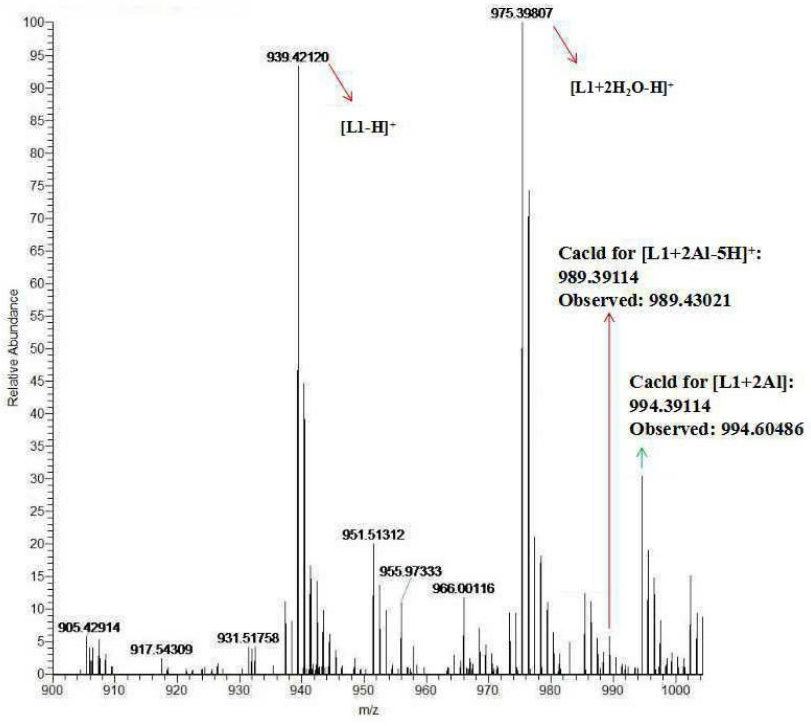

Figure S14. MALDI-TOF-MS spectrum of **L1**·2Al complex.

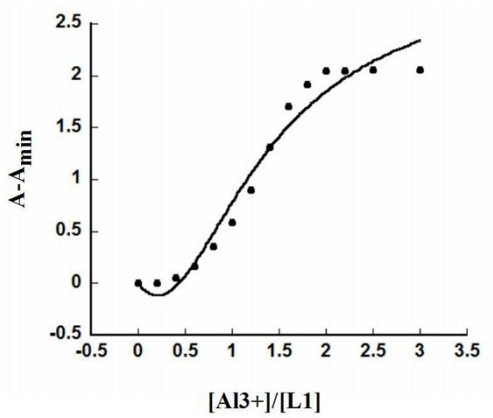

Figure S15. Non-linear plot of probe **L1** (50 μM) assuming a 1:2 stoichiometry for association between probe **L1** and Al^{3+} in CH_3CN/H_2O (v/v, 98/2, pH 7) solution by absorption spectroscopy. λ_{max} = 558 nm.[1]

The UV spectrum association constants of Al^{3+} were calculated by nonlinear fitting using the following formula [Eq. (3)]:

$$\Delta A_{Al} = \frac{\varepsilon_{\Delta HG}[H_0]K_1[G] + \varepsilon_{\Delta HG_2}[H_0]K_1K_2[G]^2}{1 + K_1[G] + K_1K_2[G]^2} \quad (3)$$

where ΔA_{Al} is the change in the UV absorption intensity of the **L1** upon gradual addition of the Al^{3+}, and $\varepsilon_{\Delta HG}$ refers to the different molar absorptivity of the free host and the complex of one host and one guest, $\varepsilon_{\Delta HG_2}$ refers to the different molar absorptivity of the free host and the complex of one host and two guests. The molar concentrations of the free guest are denoted by [H]and [G], respectively.

Equation(3) is noting also the relevant mass balance eqn (2), molar concentration of the 1 : 1 complex are denoted by [HG], [HG2] refers to 1 : 2 complex[1].

$$[H0] = [H] + [HG] + [HG2] \quad (2)$$

R= 0.9842, K_1=1225.8 (±0.312)M^{-1}, $K_2 = 2.654\times10^5$(±0.312)M^{-2}.

Reference:

[1] P. Thordarson, *Chem. Soc. Rev.*, 2011, **40**, 1305-1323.

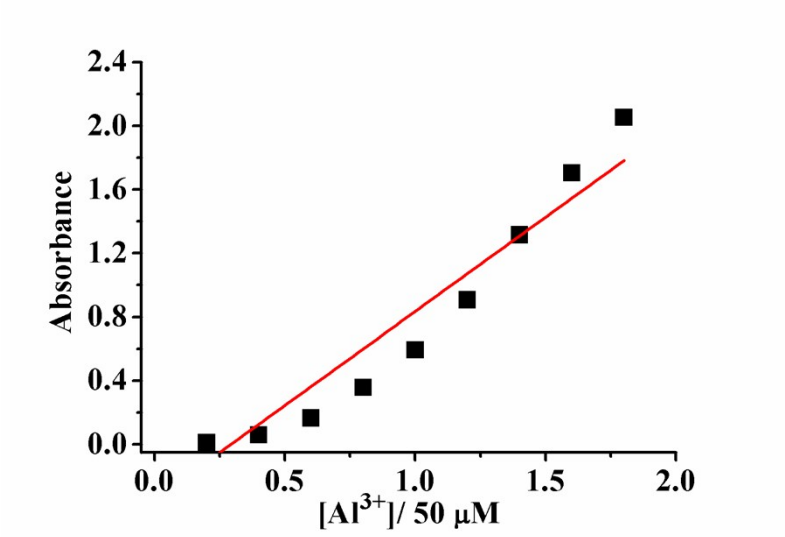

Figure S16. Absorbance calibration curve of probe **L1** (50 μM) at 558 nm as a function of Al^{3+} concentration in CH_3CN/H_2O (v/v, 98/2, pH 7) solution.

Y = 1.184 X - 0.3483, R = 0.9055, LOD = 5.8 μM.

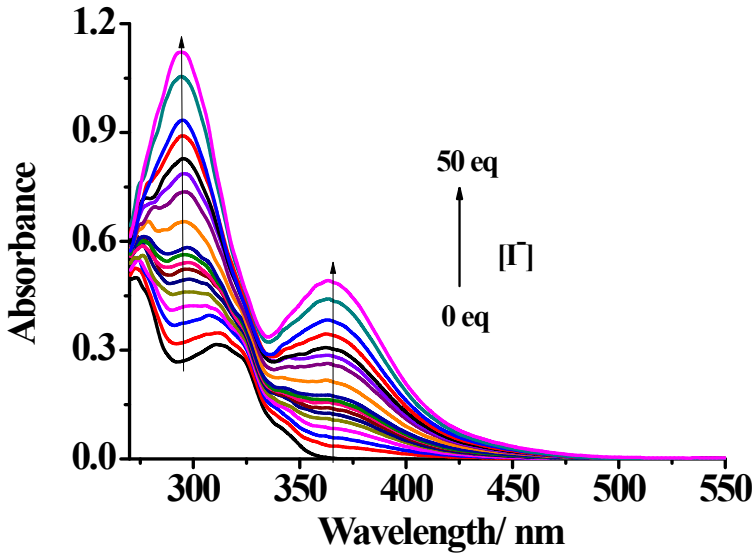

Figure S17. Absorption spectral changes of probe **L1** (10 μM, H_2O/1,4-dioxane, 1/99, v/v) solution upon addition of I^- (0 ~ 50 equiv.)

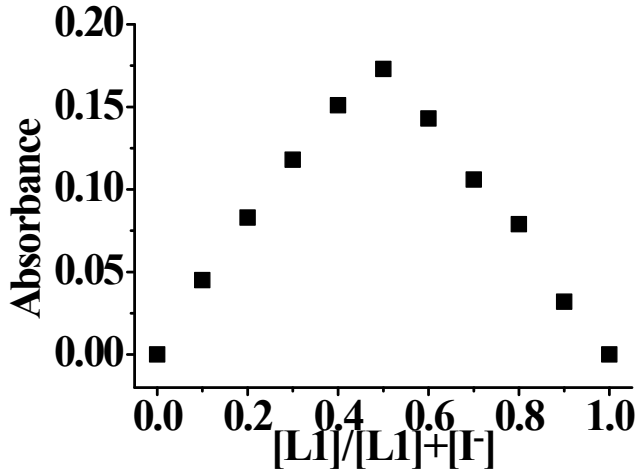

Figure S18. Job's plot data.

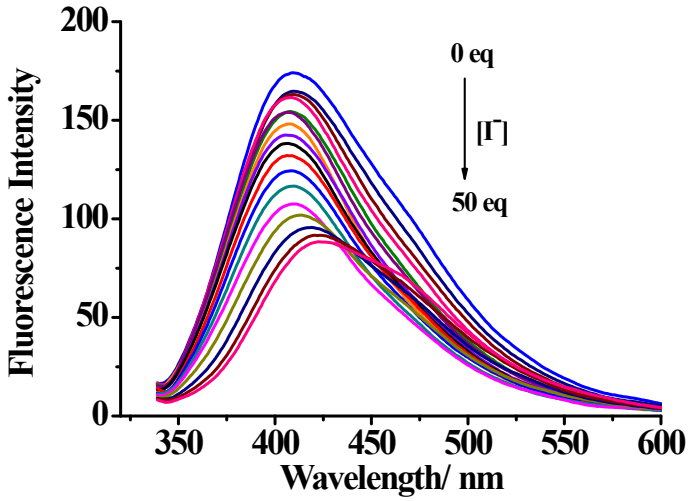

Figure S19. Fluorescence spectral changes of probe **L1** (10 μM, 1,4-dioxane/H_2O, v/v, 99/1) solution upon addition of I^- (0 ~ 500 μM); $\lambda_{ex}/\lambda_{em}$ = 315 nm/415 nm.

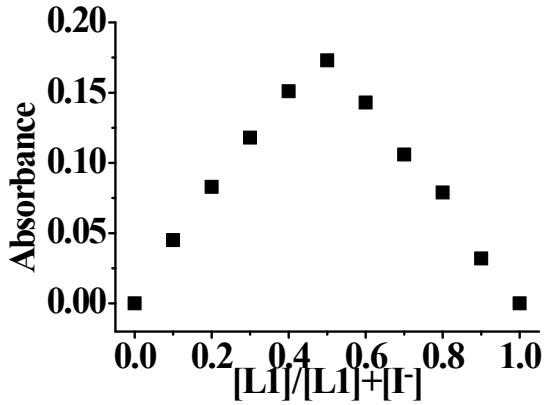

Figure S20. Job's plot data.

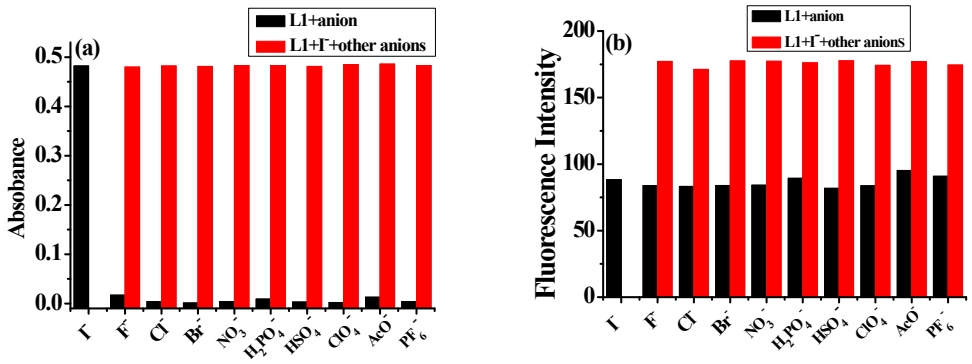

Figure S21. (a) Absorption response of probe **L1** (10 μM, 1,4-dioxane/H_2O, v/v, 99/1). Black bars: the absorbance of probe **L1** at 360 nm with the addition of the respective anions (50 eq.). White bars: the absorbance of probe **L1** at 360 nm with the addition of the respective competing anions (50 eq.) and I^- (50 eq.); (b) Fluorescence response of probe **L1** (10 μM, 1,4-dioxane/H_2O, v/v, 99/1). Black bars: emission intensity of probe **L1** at 415 nm with the addition of the respective anios (50 eq.). White bars: emission intensity of probe **L1** at 415 nm with the addition of the respective competing anions (50 eq.) and I^- (50 eq.). Anions including I^-, F^-, Cl^-, Br^-, NO_3^-, $H_2PO_4^-$, HSO_4^-, ClO_4^-, A_CO^- and PF_6^-. λ_{ex} = 315 nm

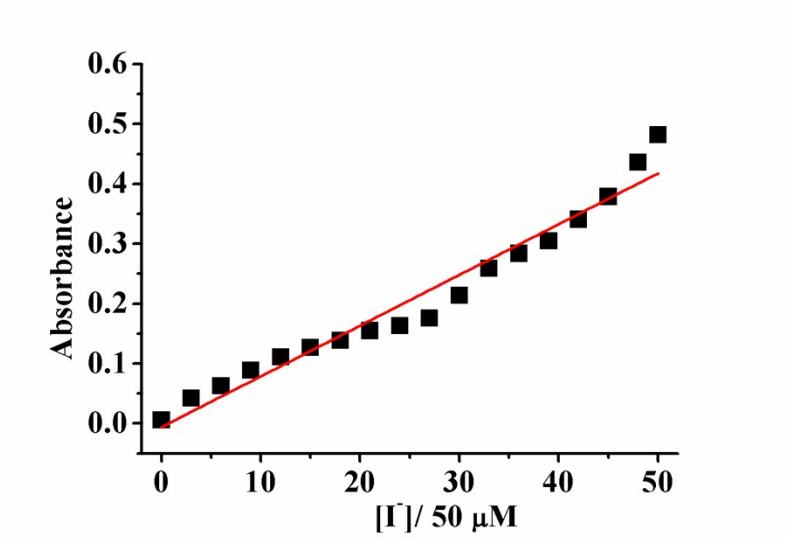

Figure S22. Absorbance calibration curve of probe **L1** (10 μM) as a function of I^- concentration in 1,4-dioxane/H_2O (v/v, 99/1) solution; λ_{max} = 360 nm.

Y = 0.00847 X - 0.00598, R = 0.9578, LOD = 0.42 μM.

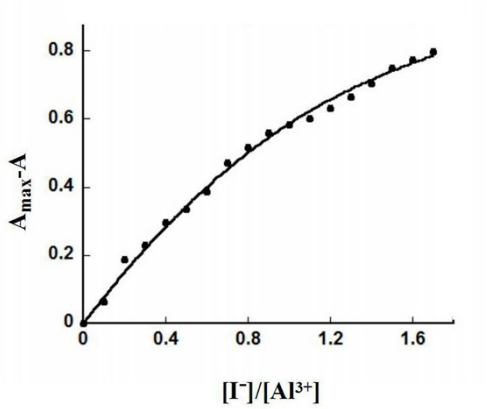

Figure S23. None-linear plot of probe **L1** (of probe **L1**(10 μM) assuming a 1:1 stoichiometry for association between probe **L1** and I^- in 1,4-dioxane/H_2O (v/v, 99/1) solution by absorption spectroscopy. λ_{max} = 360 nm.

The UV spectrum association constants of I^- were calculated by nonlinear fitting using the following formula [Eq. (4)]:

$$\Delta F = \frac{\Delta\beta([H]_0 + [G]_0 + 1/K_a) \pm \sqrt{\Delta\beta^2([H]_0 + [G]_0 + 1/K_a)^2 - 4\Delta\beta^2[H]_0[G]_0}}{2} \quad (4)$$

where ΔI is the change in the fluorescence intensity of the L1 upon gradual addition of the I^-, and Δβ refers to the different molar absorptivity of the free host and the interaction complex. The total concentrations of host and guest are denoted by $[H]_0$ and $[G]_0$, respectively[1].

R = 0.9975, K =2.08×10^5 (±0.005)M^{-1}

Reference:

[1] P. Thordarson, *Chem. Soc. Rev*., 2011, **40**, 1305-1323.

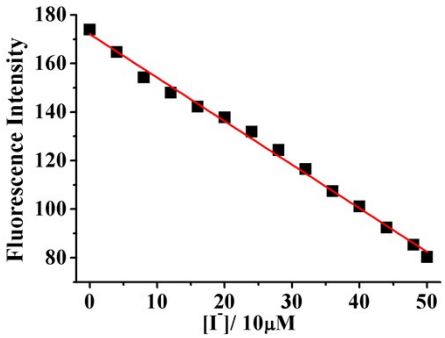

Figure S24. Fluorescence intensity calibration curve of probe **L1** (10 μM) as a function of I^- concentration in 1,4-dioxane/H_2O (v/v, 99/1) solution; $\lambda_{ex}/\lambda_{em}$ = 315 nm/415 nm.

Y = - 1.793 X + 172.1, R = 0.9953, LOD = 0.092 μM.

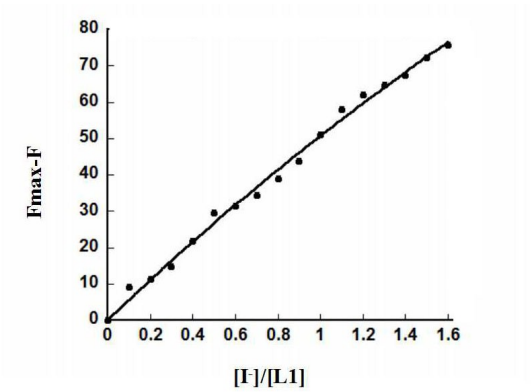

Figure S25. None-linear plot of probe**L1** (10 μM) assuming a 1:1 stoichiometry for association between probe **L1** and I^- in 1,4-dioxane/H_2O (v/v, 99/1) solution by fluorescence spectroscopy; $\lambda_{ex}/\lambda_{em}$ = 315 nm/415 nm.

The fluorescence spectrum association constants of I^- were calculated by nonlinear fitting using the following formula [Eq. (5)]:

$$\Delta I = \frac{\Delta a([H]_0 + [G]_0 + 1/K_a) \pm \sqrt{\Delta a^2([H]_0 + [G]_0 + 1/K_a)^2 - 4\Delta a^2[H]_0[G]_0}}{2} \quad (5)$$

where ΔI is the change in the fluorescence intensity of the L1 upon gradual addition of the I^-, and Δα refers to the different constant of the free host and the interaction complex. The total concentrations of host and guest are denoted by $[H]_0$ and $[G]_0$, respectively[1].

R = 0.9910, K =1.04×10^4 (±0.033)M^{-1}

Reference:

[1] P. Thordarson, *Chem. Soc. Rev.*, 2011, **40**, 1305-1323.

Table S1. Comparison of probe **L1** and other probes in literature

	Our work	Ref. [2]	Ref. [3]	Ref. [4]	Ref. [5]
Detection ions	Al^{3+}, I^-	Al^{3+}	Al^{3+}	Al^{3+}	Al^{3+}
Detection solvent (v/v)	Al^{3+}: CH_3CN/H_2O (98/2) I^-: 1,4-dioxane/H_2O (99/1)	C_2H_5OH/H_2O (9/1)	CH_3OH/H_2O (1/1)	C_2H_5OH/ H_2O(95/5)	C_2H_5OH
Yield (%)	76.3	85.2	70.2	NA	93.1
Quantum yield	Al^{3+} 0.39	NA	0.076	0.102	NA
Detection limit (μM)	Al^{3+} 0.073 I^- 0.46	1.04	0.39	NA	0.2
Detection Method	Al^{3+}: Ratiometric fluorescence Stoke's shift (345 nm); FRET I^-: Fluorescence quenching PET	Ratiometric fluorescence Stoke's shift (143 nm)	Single wavelength Stoke's shift (72 nm); ESIPT	Single wavelength Stoke's shift (65 nm); PET	Single wavelength Stoke's shift (57 nm); PET
Application	PC3 Cells	Test strips	HeLa cells	NA	NA

	Ref. [6]	Ref.[7]	Ref.[8]
Detection ions	Al^{3+}, F^-	Al^{3+}	Al^{3+}
Detection solvent (v/v)	DMSO	CH_3CN	C_2H_5OH
Yield (%)	85.0	86.1	53
Quantum yield	Al^{3+}: 0.0198 F^-: 0.0182	NA	NA
Detection limit(μM)	Al^{3+}: 0.41 F^-: 14.36	0.42	0.22
Detection Method	Single wavelength Al^{3+}: ICT F^-: hydrogen bonded	Ratiometric fluorescence Stoke's shift (75 nm); ICT	Single wavelength; PET
Application	HeLa cells	HeLa cells	NA

[2] Y. Zhang , Y. Fang , N. Z. Xu, M. Q. Zhang, G. Z. Wu and C. Yao, *Chinese Chemical Letters*., 2016, **27**, 1673–1678.

[3] D. Sarkar, A. Pramanik, S. Biswas, P. Karmakar and T. K. Mondal, *RSC Adv*., 2014, **4,** 30666-30672.

[4] S. Samanta, B. Nath and J. B. Baruah, *Inorg. Chem. Commun*., 2012, **22**, 98-100.

[5] J. C. Qin, X. Y. Cheng, K. C. Yu, R. Fang, M. F. Wang and Z. Y. Yang 2015, **7**, 6799-6803.

[6] H. Y. Jeong, S. Y. Lee, J. Han, M. H. Lim and C. Kim, *Tetrahedron*., 2017, **73**, 2690-2697.

[7] R. Patil, A. Moirangthem, R. Butcher, N. Singh, A. Basu, K. Tayade, U. Fegade, D. Hundiwale and A. Kuwar, *Dalton Trans*., 2014, **43**, 2895-2899.

[8] J. W. Jeong, B. A. Rao and Y. A. Son, *Sensor. Actuators B: Chem*., 2015, **208** , 75-84.